PHYSICAL REVIEW A **73**, 052505 (2006)

Direct observation of the $^2D_{3/2}$-$^2D_{5/2}$ ground-state splitting in Xe^{9+}

E. Takács,[1,2] B. Blagojevic,[1,*] K. Makónyi,[1] E.-O. Le Bigot,[1,3] C. I. Szabó,[1,2] Y.-K. Kim,[1] and J. D. Gillaspy[1]

[1]*National Institute of Standards and Technology, Gaithersburg, Maryland, 20899-8421, USA*

[2]*Experimental Physics Department, University of Debrecen, Bem ter 18/a, Debrecen H-4026, Hungary*

[3]*Laboratoire Kastler Brossel, CNRS, Ecole Normale Supérieure et Université Pierre et Marie Curie, 4 place Jussieu, Case 74, 75005 Paris, France*

(Received 15 March 2006; published 18 May 2006)

We have used an electron beam ion trap to observe a visible line at 598.30(13) nm that corresponds to the $4d^9\ ^2D_{3/2}-4d^9\ ^2D_{5/2}$ magnetic dipole transition within the ground state configuration of Xe^{9+}. We have found no evidence to support the claim by others that a line near this position originates from Xe^{31+}. The comparison of the measured wavelength with previous indirect experimental values, and the dependence of the line intensity on the electron beam energy, confirms the validity of the present identification. Our measured wavelength is in agreement with semiempirical Hartree-Fock calculations but shows a discrepancy with *ab initio* multiconfiguration Dirac-Fock calculations. We propose that the line may be useful as a diagnostic for extreme ultraviolet lithography light sources.

DOI: 10.1103/PhysRevA.73.052505 PACS number(s): 32.30.Jc, 31.15.Ar, 85.40.Hp, 31.30.Jv

I. INTRODUCTION

Energy level separations in the ground state configurations of multiply charged ions offer both theoretical challenges and practical plasma diagnostic applications [1–10]. Both laboratory and astrophysical plasma studies can take advantage of magnetic dipole or higher order transitions taking place within the ground term. Recent interest in extreme ultraviolet radiation (EUV) for lithographic applications by the microelectronics industry has made xenon plasmas and medium charge state xenon ions the focus of several research investigations [11]. Since the EUV lines used for these applications originate primarily from Xe^{10+} ions, visible lines in nearby charge states can provide useful diagnostics.

The energy separation between the $4d^9\ ^2D_{3/2}$ and $4d^9\ ^2D_{5/2}$ ground term levels of Rh-like xenon has been predicted theoretically and indirectly inferred from measurements at longer wavelengths by Kaufmann *et al.* [12]. The experimentally inferred value was determined from pairs of EUV transitions that originate from the same upper state, but decay to either one or the other ground state level. These high precision EUV measurements were carried out using a xenon puff triggered high voltage arc source [12]. In a later investigation, the same datasets were analyzed by Churilov *et al.* [13]. The authors were able to reduce the experimental error bars by a factor of two, but the value still remained within the estimated limits of the predicted theoretical value. Our *ab initio* calculations provide a different theoretical result that falls well outside the error bars on the experiment.

In the present work, we report the direct observation of the $4d^9\ ^2D_{3/2}$-$4d^9\ ^2D_{5/2}$ M1 transition using the electron beam ion trap (EBIT) at the National Institute of Standards and Technology. The origin of the line was definitively identified in the spectrum of multiply charged xenon by mapping out the electron energy dependence near the threshold for creating Xe^{9+} ions.

II. EXPERIMENTAL SETUP

Inside the EBIT, a high density electron beam creates multiply charged ions and assists a 3 *T* Penning trap to confine them [14]. The rather sharp longitudinal energy distribution of the electron beam allows the mapping of the energy dependence of resonant and threshold processes [15].

Visible lines emitted from the trap were analyzed using a 0.3 m Czerny-Turner grating monochromator [2] with the exit slit replaced by a charge-coupled device (CCD) detector. With the 1200 grooves per mm grating used in this investigation, the entire visible wavelength range can be covered with about five CCD images.

Neutral xenon gas was injected through a set of apertures mounted on one of the side ports of the EBIT. The electron beam energy was varied between 100 and 500 eV to map the energy region around the ionization potential of Xe^{8+}. This beam energy is relatively low compared to that for which the EBIT was designed, so it was operated with considerably less beam current (under 1 mA) than is typical at higher energies. Figure 1 shows the spectrum at 220 eV electron energy. The inset was taken with no Xe gas injection under the same EBIT conditions, thus providing evidence that the line originates from xenon. Higher electron beam energy measurements were also taken to establish the wavelength calibration as described in the following section.

III. WAVELENGTH CALIBRATION

In order to identify the $4d^9\ ^2D_{3/2}$-$4d^9\ ^2D_{5/2}$ M1 Xe^{9+} line near 598 nm, we calibrated our spectrometer using lines from a mercury spectral lamp and known lines of Xe^{1+} from the EBIT. The singly charged xenon lines were recorded at 8 keV electron beam energy with high electron beam currents (on the order of 150 mA). The lines used for the cali-

*Present address: Science and Engineering Services, Inc., 6992 Columbia Gateway Dr., Columbia, MD 21046.

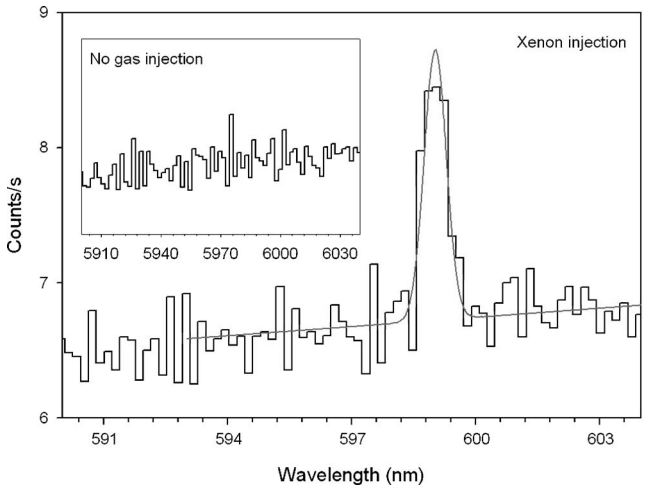

FIG. 1. Spectrum around the 598 nm region with and without xenon gas injection at 220 eV electron impact energy.

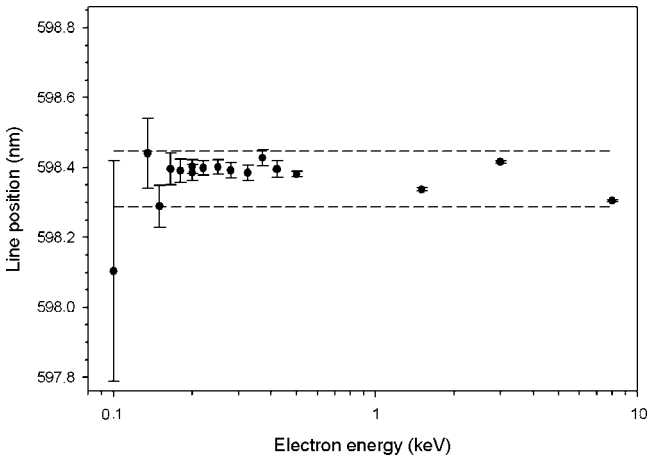

FIG. 2. Line positions at different electron impact energies. One-sigma statistical uncertainties are shown as error bars on the individual points; the estimated systematic uncertainty is 0.08 nm.

bration were chosen to lie on both sides of the candidate transition. Their wavelengths were taken from Ref. [16];

$$\text{Xe II}(^1\text{D})5d\ ^2\text{D}_{5/2}\text{-}(^1\text{D})6p\ ^2\text{P}^\text{o}_{3/2}\text{:589.329 nm},$$

$$\text{Xe II}(^1\text{D})6s\ ^2\text{D}_{3/2}\text{-}(^1\text{D})6p\ ^2\text{P}^\text{o}_{3/2}\text{:597.113 nm},$$

$$\text{Xe II}(^3\text{P})5d\ ^4\text{D}_{5/2}\text{-}(^3\text{P})6p\ ^4\text{P}^\text{o}_{5/2}\text{:603.620 nm},$$

$$\text{Xe II}(^3\text{P})5d\ ^4\text{D}_{7/2}\text{-}(^3\text{P})6p\ ^4\text{P}^\text{o}_{5/2}\text{:605.115 nm},$$

$$\text{Xe II}(^3\text{P})5d\ ^4\text{D}_{5/2}\text{-}(^3\text{P})6p\ ^4\text{P}^\text{o}_{3/2}\text{:609.759 nm}.$$

The strong mercury lines at 576.96 nm and 579.067 nm wavelengths [17] helped to establish the wavelength calibration across the whole region observed on a single CCD image. The mercury lamp situated on the EBIT observation port opposite to the grating spectrometer was focused into the position of the electron beam in the center of the machine. This setup allowed us to observe the mercury lines without any change in the spectrometer or in the optical setup used for the measurement of the lines from the EBIT. The CCD channels were calibrated for wavelength using a second order polynomial function.

As part of our assessment of the systematic errors, we compared the wavelengths of the $4d^9\ ^2\text{D}_{3/2}$-$4d^9\ ^2\text{D}_{5/2}$ line determined at different electron beam energies and at different gas pressures. Figure 2 shows the line positions at different electron beam energies. Our estimate for a possible systematic error is 0.08 nm. The uncertainty from the wavelength calibration and the statistical uncertainty in the line position is 0.1 nm. Our overall combined uncertainty for the $4d^9\ ^2\text{D}_{3/2}$-$4d^9\ ^2\text{D}_{5/2}$ line position is 0.13 nm.

IV. RESULTS

Table I shows the separation of the $4d^9\ ^2\text{D}_{3/2}$ and $4d^9\ ^2\text{D}_{5/2}$ levels in Xe^{9+}. Our experimental result is 598.30(13) nm and it is slightly higher than the indirect measurement by Churilov *et al.* The two results agree, however, to within their error limits.

The theoretical calculations shown in Table I are semiempirical Hartree-Fock values obtained by Kaufman *et al.* [12] and our present multiconfiguration Dirac-Fock (MCDF) result. The authors of the semiempirical Hartree-Fock calculations estimated a 0.7 nm uncertainty in their results based on fits to ground term experimental data along the Rh-like isoelectronic sequence. Their values are in reasonable agreement with the experimental results. Our *ab inito* MCDF calculation predicts a longer 605.07 nm wavelength and shows a larger discrepancy with the measured data. Details about the theoretical calculations are given in the next section.

There have been reports in the literature of another line in this wavelength region observed with the Livermore EBIT at higher electron beam energies. However, this line was identified as a transition within the ground term configuration of Xe^{31+} [18,19]. The reported 598.40(100) nm wavelength is the same as our measured 598.30(20) nm value for the $4d^9\ ^2\text{D}_{3/2}$-$4d^9\ ^2\text{D}_{5/2}\text{Xe}^{9+}$ transition, to within the experimental uncertainties. Our measurement for the energy dependence of the line intensity rules out that the line we observed

TABLE I. Experimental and theoretical values for the $4d^9\ ^2\text{D}_{3/2}$-$4d^9\ ^2\text{D}_{5/2}$ splitting in Xe^{9+}.

Transition	Experiment		Theory	
$4d^9\ ^2\text{D}_{3/2}$–$4d^9\ ^2\text{D}_{5/2}$	Churilov *et al.* [3]	This work	HF (semi-empirical) Kaufman *et al.* [2]	MCDF Kim [4]
	597.91(36) nm	598.30(13) nm	597.37 nm	605.07 nm

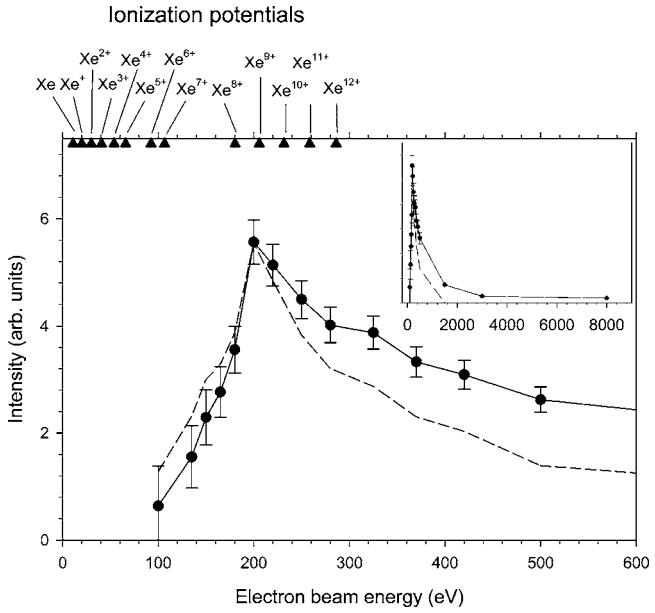

FIG. 3. Electron beam energy dependence of the intensity of the Xe line measured at 598.30(13) nm wavelength. The data are normalized to the electron beam current. The dashed line shows a normalization of the data to the square of the electron beam current. The correct normalization should lie somewhere between these two limits. The inset shows the energy range extended to 8 keV. Error bars are at the one-sigma level.

originates from Xe^{31+}, however, since it appears at electron energies well below the ionization threshold for Xe^{30+}. The energy dependence of our measured line intensity is shown in Fig. 3. The dependence is in accordance with the assumption that the line originates only from Xe^{9+}.

V. THEORETICAL

The semiempirical Hartree-Fock value by Kaufman *et al.* [12] quoted in Table I (597.37 nm±0.71 nm) was obtained by using the ratios between the Hartree-Fock value of the spin-orbit radial integral ς_d and the values of the integral obtained by fitting the experimental data for Ag III through Cs XI. They concluded that the fine-structure splitting in Xe X was 597.56±0.71 nm based on the differences in the experimental wavelengths.

The wavelength of 598.30 nm corresponds to 16709 cm^{-1} in wave number. The theoretical wave number calculated from Dirac-Fock wave functions without taking into account electron correlation is 16532 cm^{-1}, while the wave number from multiconfiguration Dirac-Fock (MCDF) wave functions is 16 488 cm^{-1}. For the MCDF calculation, we have used a relativistic equivalent of two nonrelativistic correlation configurations—$4d^7 5p^2$ and $4d^7 4f^2$—in addition to the reference configuration of $4d^9$. The fact that the answer from the correlated wave functions is less accurate than that from the uncorrelated wave functions is an indication that many more correlation configurations must be used.

The calculation of this fine-structure splitting involves taking the difference between the total energies of the two fine-structure levels. Five significant figures are lost in the subtraction because the individual total energies are large in magnitude while the difference is small. To match the experimental wave number, MCDF calculations must include all configurations that may affect the total energies in the eighth and ninth significant figures. The MCDF code we have used [20] produced total energies converged to nine significant figures in the three-configuration calculation mentioned above. It will be necessary to include tens of thousands of relativistic configurations in MCDF calculations involving orbitals of high principal quantum numbers as well as core-excited configurations to achieve the required accuracy. Such a massive MCDF calculation is beyond the scope of the present study.

VI. CONCLUSION

We have observed and identified the $4d^9\ ^2D_{3/2}$-$4d^9\ ^2D_{5/2}$ magnetic dipole transition in Xe^{9+}. The wavelength of this transition is 598.30(13) nm. Our results are in agreement with a previous indirect determination of the splitting of the $4d^9\ ^2D_{3/2}$ and $4d^9\ ^2D_{5/2}$ levels. An *ab initio* MCDF calculation fails to describe the measured wavelength. We see no evidence for a line at this wavelength from Xe^{31+}, and conclude that it was likely misidentified in previous reports [18,19]. Because the charge state of this line is much lower than previously reported, we propose that it be used for remote diagnostics of EUV lithography light sources that operate primarily on the neighboring charge state, Xe^{10+}.

ACKNOWLEDGMENTS

This work was supported in part by funding from International SEMATECH and the U.S. Department of Energy, Office of Fusion Energy Science. The authors would like to thank Dr. Joseph Reader for discussions. E.T. was partially supported by a grant from the Hungarian Science Fund (Grant No.: OTKA T046454).

[1] C. A. Morgan, F. G. Serpa, E. Takács, E. S. Meyer, J. D. Gillaspy, J. Sugar, J. R. Roberts, C. M. Brown, and U. Feldman, Phys. Rev. Lett. **74**, 1716 (1995).

[2] F. G. Serpa, E. S. Meyer, C. A. Morgan, J. D. Gillaspy, J. Sugar, and J. R. Roberts, Phys. Rev. A **53**, 2220 (1996).

[3] H. Adler, E. S. Meyer, F. G. Serpa, E. Takács, J. D. Gillaspy, C. M. Brown, and U. Feldman, Nucl. Instrum. Methods Phys. Res. B **98**, 581 (1995).

[4] S. B. Utter, P. Beiersdorfer, and E. Traebert, Phys. Rev. A **67**, 012508 (2003).

[5] E. Traebert, P. Beiersdorfer, S. B. Utter, and J. R. Crespo Lopez-Urrutia, Phys. Scr. **58**, 599 (1998).

[6] H. Watanabe, D. Crosby, F. J. Currell, T. Fukami, D. Kato, S. Ohtani, J. D. Silver, and C. Yamada, Phys. Rev. A **63**, 042513 (2001).
[7] D. N. Crosby, K. Gaarde-Widdowson, J. D. Silver, and M. R. Tarbutt, Phys. Scr., T **92**, 144 (2001).
[8] P. Indelicato, Phys. Scr., T **65**, 57 (1996).
[9] R. Doron and U. Feldman, Phys. Scr. **64**, 319 (2001).
[10] D. R. Beck, Phys. Rev. A **60**, 3304 (1999).
[11] K. Fahy, P. Dunne, L. McKinney, G. O'Sullivan, E. Sokell, J. White, A. Aguilar, J. M. Pomeroy, J. N. Tan, B. Blagojevic, E.-O. LeBigot, and J. D. Gillaspy, J. Phys. D **37**, 3225 (2004).
[12] V. Kaufman, J. Sugar, and J. L. Tech, J. Opt. Soc. Am. **73**, 691 (1983).
[13] S. S. Churilov and Y. N. Joshi, Phys. Scr. **65**, 40 (2004).
[14] *Highly Charged Ions: Publications of the EBIT Project*, 1993-2001, edited by J. D. Gillaspy, L. P. Ratliff, J. R. Roberts, and E. Takács, National Institute of Standards and Technology Special Publication 972 (U.S. Government Printing Office, Washington, 2002).
[15] D. J. McLaughlin, Y. Hahn, E. Takács, E. S. Meyer, and J. D. Gillaspy, Phys. Rev. A **54**, 2040 (1996).
[16] D. R. Lide, *CRC Handbook of Chemistry and Physics, 84th Edition* (CRC Press, Boca Raton, 2003) pp. 10-145.
[17] C. J. Sansonetti, M. L. Salit, and J. Reader, Appl. Opt. **35**, 74 (1996).
[18] J. R. Crespo Lopez-Urritia, P. Beiersdorfer, K. Widman, and V. Decaux, Phys. Scr., T **80**, 448 (1999).
[19] J. R. Crespo Lopez-Urritia, P. Beiersdorfer, K. Widman, and V. Decaux, Can. J. Phys. **80**, 1687 (2002).
[20] J. P. Desclaux and P. Indelicato, http://dirac.spectro.jussieu.fr/mcdf